L-Lactide Polymerization Utilizing a Hydroxy-Functionalized 3,6-Bis(2-pyridyl)pyridazine as Supramolecular (Co)initiator: Construction of Polymeric [2 × 2] Grids

Richard Hoogenboom, Daan Wouters, and Ulrich S. Schubert*

Laboratory of Macromolecular Chemistry and Nanoscience, Eindhoven University of Technology and Dutch Polymer Institute (DPI), PO Box 513, 5600 MB Eindhoven, The Netherlands

Received January 29, 2003; Revised Manuscript Received April 25, 2003

ABSTRACT: A hydroxy-functionalized 3,6-bis(2-pyridyl)pyridazine ligand was synthesized from 3,6-bis-(2-pyridyl)tetrazine and 5-hexyn-1-ol. This ligand was subsequently polymerized with L-lactide utilizing a controlled aluminum alkoxide-based polymerization. The resulting poly(L-lactide) macroligands were characterized with ^{1}H NMR spectroscopy, IR spectroscopy, gel permeation chromatography, and MALDI-TOF-MS, revealing the successful incorporation of the ligand into the polymer chains. Complexation studies of both the hydroxy-functionalized ligand and the macroligands were performed by UV−vis spectroscopic investigations, demonstrating the exclusive formation of metallo-supramolecular gridlike architectures. In addition, AFM measurements also revealed the existence of the defined polymeric species.

Introduction

In recent years, well-defined (block co)polymers have attracted significant attention for obtaining novel nanostructures like micelles[1−3] and controlled architectures.[4,5] Moreover, the introduction of supramolecular interactions into defined polymeric systems can lead to materials combining interesting (responsive) architectures with new mechanical and physical properties.[6,7] Besides hydrogen-bonding and ionic interactions, metal−ligand interactions are of central interest. Supramolecular metal coordinating units can be introduced into polymeric systems by utilizing functionalized monomers,[8−10] end group,[11,12] or side group[13,14] functionalization as well as by utilizing functional initiators and/or functionalized end-cappers for living or controlled polymerizations.[15−18] The functional initiator approach for living polymerizations seems to be the most promising, since all polymer chains contain a connected metal coordinating unit after purification of the polymer. By introducing more initiating groups onto the central metal complex, a wide variety of linear and star-shaped polymers are accessible.[15,19] Furthermore, the nature of the polymers can be controlled by utilizing different monomers and polymerization techniques. In addition, block copolymers are easily accessible by the stepwise addition of different monomers. So far, the feasibility of this approach has been successfully demonstrated for bipyridine and terpyridine systems utilizing controlled radical polymerizations,[16] living cationic ring-opening polymerizations of 2-oxazolines,[15,17,20−22] and the controlled polymerization of lactides and lactones.[15,17,18] To extend this approach to larger as well as higher organized architectures, grid-forming ligands can be utilized instead of bipyridine and terpyridine moieties: Gridlike complexes containing up to 20 ligands (e.g., [2 × 2],[23,24] [2 × 3],[25,26] [3 × 3],[27,28] [4 × 4],[29] and [4 × 5][30]) have been reported, whereas simple terpyridine and bipyridine units can form complexes with only two or three ligands, respectively. The incorporation of these grid-forming ligands into polymers seems to be very promising since materials with properties of both the gridlike metal complexes (e.g., (reversible) self-assembly of up to 20 polymer chains, special magnetic, electrochemical, and optical properties) and polymers (e.g., film forming and good solubility) can be obtained. Furthermore, the complexation strength as well as the size and amount of polymer chains can be adjusted in these supramolecular polymers by utilizing different grid-forming ligands and metal salts. Up to now, the incorporation of such grid-forming ligands into macromolecules has been unexplored. In this contribution, we describe the polymerization of L-lactide utilizing a novel supramolecular initiating system based on the 3,6-bis(2-pyridyl)pyridazine ligand. For this purpose, a hydroxy-functionalized 3,6-bis(2-pyridyl)pyridazine was synthesized and polymerized. The resulting macroligands were assembled into gridlike complexes with copper(I) ions as described 10 years ago in the literature for an unsubstituted 3,6-bis(2-pyridyl)pyridazine (Figure 1).[23]

Experimental Section

Materials. Solvents were purchased from Biosolve; 5-hexyn-1-ol (96%), tetrakis(acetonitrile)copper(I) hexafluorophosphate (no purity given, but fitting elemental analysis in certificate of analysis), triethylaluminum (1.9 M in toluene), and L-lactide (98%) were obtained from Aldrich. Toluene was dried over Al_2O_3 (Merck, neutral standard) before usage. L-Lactide was recrystallized from ethyl acetate and stored over P_2O_5. All other compounds were used without further purification. 3,6-Bis(2-pyridyl)tetrazine (**1**) was synthesized as described in the literature.[31]

Instruments. ^{1}H NMR and ^{13}C NMR were recorded on a Varian AM-400 spectrometer or a Varian Gemini 300 spectrometer. Chemical shifts are given in ppm relative to TMS for proton and carbon spectra. UV−vis spectroscopy was performed on a Perkin-Elmer Lambda 45 apparatus. IR spectra were recorded on a Perkin-Elmer 1600 FT-IR. MALDI-TOF-MS was performed on a Voyager-DE PRO Biospectrometry Workstation (Applied Biosystems) time-of-flight mass spectrometer using 5×10^{-7} bar pressure, a voltage of 25 kV, a frequency of 3.0 Hz, and linear mode for operation. The spectra were obtained in the positive ion mode, and ionization was performed with a 337 nm pulsed nitrogen laser (varying laser intensities for the different compounds). The samples

* Corresponding author: e-mail u.s.schubert@tue.nl.

10.1021/ma034119e CCC: $25.00
Published on Web 06/03/2003

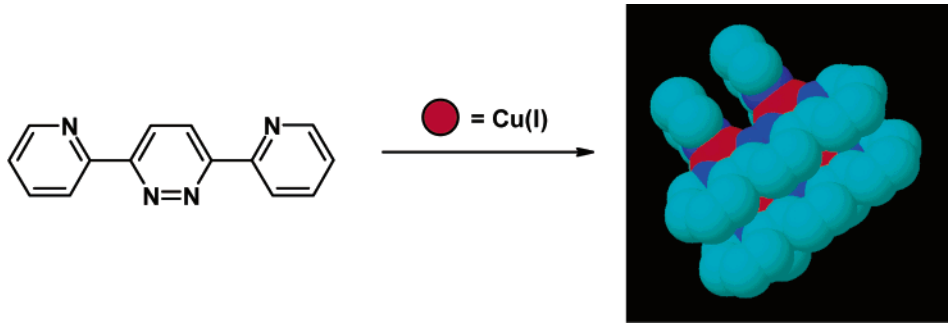

Figure 1. Complexation of the 3,6-bis(2-pyridyl)pyridazine ligand with copper(I) ions into gridlike complexes (protons omitted for clarity).

were prepared via the dried droplet multilayer spotting technique, whereby sequentially a layer of dithranol (20 mg/mL) and analyte (10 mg/mL) were spotted (no additional salt).[32] Data were processed using the Data Explorer software package (Applied Biosystems). Gel permeation chromatography (GPC) was measured on a Shimadzu system equipped with a SCL-10A system controller, a LC-10AD pump, a RID-6A refractive index detector, a SPD-10AV UV-detector at 254 nm, and a PLgel 5 μm Mixed-D column at ambient temperature (mixed pore sizes, separation range 200 Da−400 kDa), whereby chloroform was used as eluent at a flow rate of 1 mL/min. The molecular weights were calculated against polystyrene standards. AFM imaging was performed on a multimode scanning probe microscope by Digital Instruments (DI, Santa Barbara, CA). Images were obtained in tapping mode with silicon tips (NSG11, obtained from NT-MDT).

Synthesis. 3,6-Bis(2-pyridyl)-4-(1-hydroxybutyl)pyridazine (6). A solution of 3,6-bis(2-pyridyl)tetrazine (**1**, 500 mg, 2.1 mmol) and 5-hexyn-1-ol (410 mg, 4.2 mmol) in toluene (25 mL) was refluxed for 40 h. After evaporation of the solvent under reduced pressure, the crude product was purified by column chromatography (Al_2O_3, chloroform as eluent). Recrystallization from chloroform:ether:hexane (1:2:1) yielded the product as a white solid (448 mg, 70%).

^{1}H NMR ($CDCl_3$): δ 8.79−8.70 (m, 3H, H-6,3″,6″), 8.48 (s, 1H, H-5′), 8.15 (d, J = 8.2 Hz, 1H, H-3), 7.88 (dt, J = 7.7, 2.2 Hz, 2H, H-4,4″), 7.40 (dt, J = 8.2, 2.2 Hz, 2H, H-5,5″), 3.62 (q, J = 4.9 Hz, 2H, CH_2OH), 3.08 (t, J = 8.2 Hz, 2H, CCH_2), 2.01 (t, J = 4.9 Hz, 1H, OH), 1.78 (quintet, J = 8.2 Hz, 2H, CH_2CH$_2$OH), 1.62 (quintet, J = 7.2 Hz, 2H, CCH$_2$CH_2).

^{13}C NMR ($CDCl_3$): δ 158.7 (C-3′), 157.0 (C-6′), 155.9 (C-2), 153.1 (C-2″), 149.1 (C-6″), 148.3 (C-6), 142.4 (C-4′), 137.0 (C-4), 136.8 (C-4″), 125.5 (C-5′), 124.7 (C-3), 124.5 (C-5), 123.5 (C-5″), 121.6 (C-3″), 61.5 (*C*H$_2$OH), 31.5 (*C*CH$_2$), 31.4 (CCH$_2$-*C*H$_2$), 25.8 (*C*H$_2$CH$_2$OH).

IR (ATR): ν = 3460 (OH stretch), 3063 (CH$_2$ stretch), 3017 (CH$_2$ stretch), 2930 (CH$_2$ stretch), 2864 (CH$_2$ stretch), 1580 (C=N stretch), 1410 (CH$_2$ deformation), 1398 (CH$_2$ deformation), 1054 (CH deformation), 1030 (C−O stretch), 991 (CH deformation), 798 (CH$_2$−(CH$_2$)$_3$ vibration), 784 (CH deformation), 746 (CH deformation), 730 (CH deformation).

MALDI-TOF-MS: m/z [M$^+$] 307 (100%). UV−vis (chloroform): λ_{max} 288 nm.

Copper(I) Grid of 3,6-Bis(2-pyridyl)-4-hydroxybutylpyridazine (4). Both **3** (10.0 mg, 30.2 mmol) and tetrakis(acetonitrile)copper(I) hexafluorophosphate (11.3 mg, 30.2 mmol) were dissolved in acetone-d_6 (1.0 mL). The resulting brown mixture was analyzed by NMR spectroscopy, and subsequently the solvent was removed under reduced pressure, yielding complex **4** as a brown solid (quantitative).

^{1}H NMR (acetone-d_6): δ 9.10−8.95 (m, 4H, H-5′), 8.60−7.90 (m, 24H, H-3,3″,4,4″,6,6″), 7.58−7.29 (m, 8H, H-5,5″), 3.79 (m, 8H, CH_2OH), 3.38 (m, 8H, CCH_2), 2.18 (m, 8H, CH_2CH$_2$OH), 1.86 (m, 8H, CCH$_2$CH_2).

IR (ATR): ν = 1596 (C=N stretch), 1463 (CH$_2$ deformation), 1445 (CH$_2$ deformation), 1389 (CH$_2$ deformation), 1053 (C−O stretch), 1015 (CH deformation), 832 (PF_6), 785 (CH deformation), 740 (CH deformation).

MALDI-TOF-MS: [M$^+$] 307 (32%, L + H$^+$), 329 (40%, L + Na$^+$), 675 (28%, 2L + Cu(I) + H$^+$). UV−vis (methanol): λ_{max} 439 nm, 294 nm.

Poly(L-lactide) Macroligand (5). The polymerization was performed in silanized Schlenk tubes under an argon atmosphere. Compound **3** (36 mg, 0.12 mmol) was dissolved in dry toluene (5.0 mL) and cooled to 0 °C. Triethylaluminum (1.9 M, 62 μL, 0.12 mmol) was added dropwise, and the reaction mixture was allowed to warm to ambient temperature. Subsequently, L-lactide (392 mg, 2.7 mmol) was added, the reaction tubes were sealed, and the mixture was stirred for 20 h at 80 °C. The polymerization was quenched with 5 drops of water, and the desired polymer **5** (285 mg, 67%) was obtained by precipitation in ice-cold methanol.

^{1}H NMR ($CDCl_3$): δ 8.79−8.70 (m, 3H, H-5,3″,5″), 8.48 (s, 1H, H-5′), 8.15 (d, J = 8.1 Hz, 1H, H-3), 7.88 (t, J = 6.9 Hz, 2H, H-4,4″), 7.4 (t, J = 6.7 Hz, 2H, H-4,4″), 5.22−5.1 (q, J = 6.4 Hz, 49H, CHCH$_3$), 4.38 (m, 1H, CHOH) 4.12 (m, 2H, CH_2O), 3.08 (m, 2H, CCH_2), 2,78 (m, 1H, OH), 1.76−1.4 (d, J = 7.2 Hz, 307H, CCH$_2$CH_2CH_2 + CHCH_3 + H$_2$O).

IR (ATR): ν = 2998 (CH$_3$ stretch), 2948 (CH$_3$ stretch), 1756 (C=O stretch), 1586 (C=N stretch) 1456 (CH$_3$ deformation), 1360 (CH$_3$ deformation), 1182 (C−O stretch), 1131 (C−C vibration), 1088 (C−C vibration), 1044 (C−C vibration).

GPC (chloroform, UV-detector): M_n = 4911, M_w = 5921, PDI = 1.20.

Poly(L-lactide) Macroligand (6). Same procedure as for polylactide **5** but with the following amounts of reagents: **3** (16.5 mg, 0.050 mmol), toluene (5.0 mL), triethylaluminum (1.9 M, 26.3 μL, 0.050 mmol), and L-lactide (360 mg, 2.5 mmol). Yield: 351 mg, 93%.

^{1}H NMR ($CDCl_3$): δ 8.79−8.70 (m, 3H, H-5,3″,5″), 8.48 (s, 1H, H-5′), 8.15 (d, J = 7.3 Hz, 1H, H-3), 7.88 (t, J = 7.1 Hz, 2H, H-4,4″), 7.4 (t, J = 6.3 Hz, 2H, H-4,4″), 5.22−5.1 (q, J = 7.4 Hz, 90H, CHCH$_3$), 4.38 (m, 1H, CHOH) 4.12 (m, 2H, CH_2OH), 3.08 (m, 2H, CCH_2), 2,78 (m, 1H, OH), 1.76−1.4 (d, J = 6.5 Hz, 368H, CCH$_2$CH_2CH_2 + CHCH_3 + H$_2$O).

IR (ATR): ν = 2998 (CH$_3$ stretch), 2947 (CH$_3$ stretch), 1756 (C=O stretch), 1586 (C=N stretch), 1456 (CH$_3$ deformation), 1360 (CH$_3$ deformation), 1182 (C−O stretch), 1130 (C−C vibration), 1086 (C−C vibration), 1044 (C−C vibration).

GPC (chloroform, UV-detector): M_n = 9641, M_w = 11 723, PDI = 1.21.

UV−Vis Titration. A stock solution (3.0 mL) of the macroligand in dichloromethane (**5**: 0.50 mg/mL; **6**: 1.0 mg/mL) was transferred into a quartz UV cuvette. Small portions (25 or 22 μL for **5** and **6**, respectively) of a stock solution of tetrakis(acetonitrile)copper(I) hexafluorophosphate in dichloromethane (0.45 mg/mL) were added stepwise to this solution, and the mixtures were shaken for several seconds. After each addition, an UV−vis spectrum was recorded.

AFM Measurements. For the AFM measurements, a solution of the copper complex of **5** in chloroform (0.050 mg/mL) was drop-cast onto mica. The measurements were performed in tapping mode.

Scheme 1. Synthesis of 3,6-Bis(2-pyridyl)-4-hydroxybutylpyridazine (3) by a Diels−Alder Reaction between 3,6-Bis(2-pyridyl)tetrazine (1) and 5-Hexyn-1-ol (2)

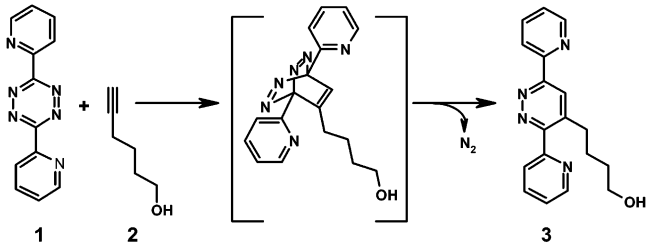

Results and Discussion

Metallo-supramolecular materials obtained significant interest during the past years.[7] To date, mainly materials based on bipyridine and terpyridine moieties were studied, whereby these ligands were mostly incorporated into macromolecules. In contrast, grid-forming ligands, such as the 3,6-bis(2-pyridyl)pyridazine ligand, which self-assemble into complexes with four ligands and four copper(I) ions,[23] have only been studied as isolated (normally crystalline) materials. Intensive efforts have been described in order to construct larger and larger systems (at present up to [4 × 5] grids)[30] in order to arrange such architectures on surfaces[33] as well as interfaces[34] and to obtain film-forming materials.[34] In all cases an elongation of the organic ligand has been utilized. Here we report a different strategy: incorporation of the grid-forming ligand into defined macromolecules.

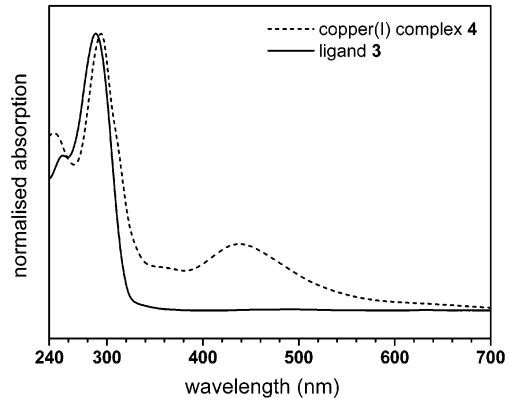

Figure 2. UV−vis spectra of ligand **3** (chloroform) and gridlike complex **4** (methanol).

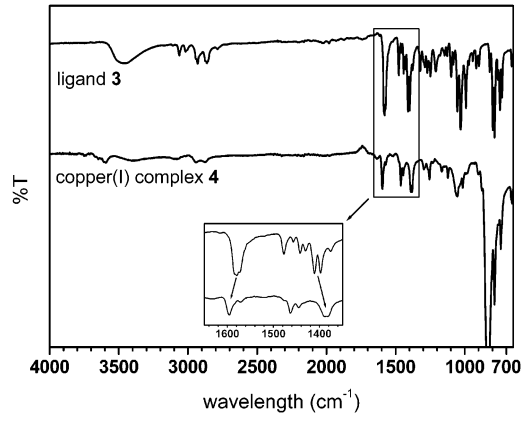

Figure 3. FT-IR spectra of ligand **3** and copper(I) complex **4**. The inset shows the characteristic shifts upon complexation.

Scheme 2. Polymerization of Ligand 3 Resulting in Macroligands 5 and 6

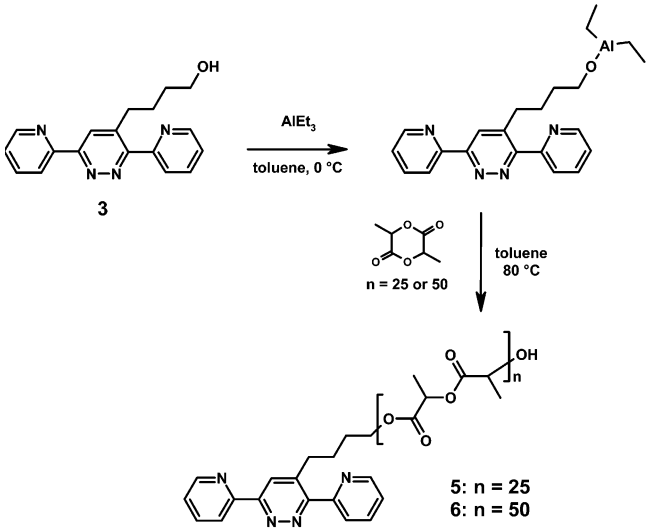

A hydroxy-functionalized 3,6-bis(2-pyridyl)pyridazine was synthesized by a Diels−Alder reaction between 3,6-bis(2-pyridyl)tetrazine (**1**) and 5-hexyn-ol (**2**), whereby elimination of a nitrogen molecule resulted in the desired 3,6-bis(2-pyridyl)-4-hydroxybutylpyridazine (**3**) (Scheme 1). ^{1}H NMR spectroscopy revealed the successful attachment of the butanol side chain to the 3,6-bis(2-pyridyl)pyridazine, whereby the OH group appeared as a quartet at 3.6 ppm. Furthermore, the asymmetry of the molecule was demonstrated by the different chemical shifts of the aromatic 3 and 3″ protons. IR spectroscopy also revealed the CH_2 groups at around 3000 cm^{-1}, and the C═N valence vibrations of the aromatic ring appeared as a broad band at 1580 cm^{-1}.

Complexation of this ligand **3** with copper(I) ions into the gridlike complex **4** was first investigated before continuing with the polymerization (Figure 1). Ligand **3** and tetrakis(acetonitrile)copper(I) hexafluorophosphate were dissolved in acetone-d_6, resulting in an instant color change from colorless to dark brown. This self-assembly was also suggested by UV−vis (Figure 2) and IR spectroscopy (Figure 3). Upon addition of 1 equiv of copper(I) ions to ligand **3**, the absorption maximum at 288 nm shifted to 294 nm and a second absorption maximum appeared at 439 nm. Both these features were also reported for the complexation of the unsubstituted 3,6-bis(2-pyridyl)pyridazine with copper(I) ions into gridlike complexes,[23] indicating that a similar gridlike complex **4** is indeed formed. With IR spectroscopy a shift from 1580 to 1596 cm^{-1} for the C═N valence vibrations of the heterocycles was observed (see inset Figure 3), and a strong band at 840 cm^{-1} for the PF_6 vibrations appeared upon complexation. The C═N valence vibrations around 1600 cm^{-1} were also reported for the unsubstituted grid complexes with other counterions.[23] In addition, the characteristic bands for the OH stretch vibrations (3460 cm^{-1}), CH_2 stretch vibrations (3063, 3017, 2930, and 2864 cm^{-1}), and CH_2 deformations (1410 and 1398 cm^{-1}) of ligand **3** become broader and weaker upon complexation whereby also the two distinct bands at 1410 and 1398 cm^{-1} merge together to form one broad band at 1389 cm^{-1} (see inset of Figure 3).

3,6-Bis(2-pyridyl)-4-hydroxybutylpyridazine (**3**) was then subsequently utilized as co-initiator for the controlled polymerization of L-lactide as described by

Table 1. Molecular Weight Data Obtained from ^{1}H NMR Spectroscopy, GPC and MALDI-TOF-MS for the Poly(L-lactide) Macroligands 5 and 6 (Values Given in daltons)

			GPC UV detector			GPC RI detector			MALDI-TOF-MS		
	$M_{n,th}$	$M_{n,NMR}$	M_n	M_w	PDI	M_n	M_w	PDI	M_n	M_w	PDI
macroligand **5**	3900	3840	4900	5900	1.20	5300	6300	1.18	2975	3624	1.12
macroligand **6**	7500	6800	9600	11700	1.21	10700	13100	1.22	5043	5602	1.11

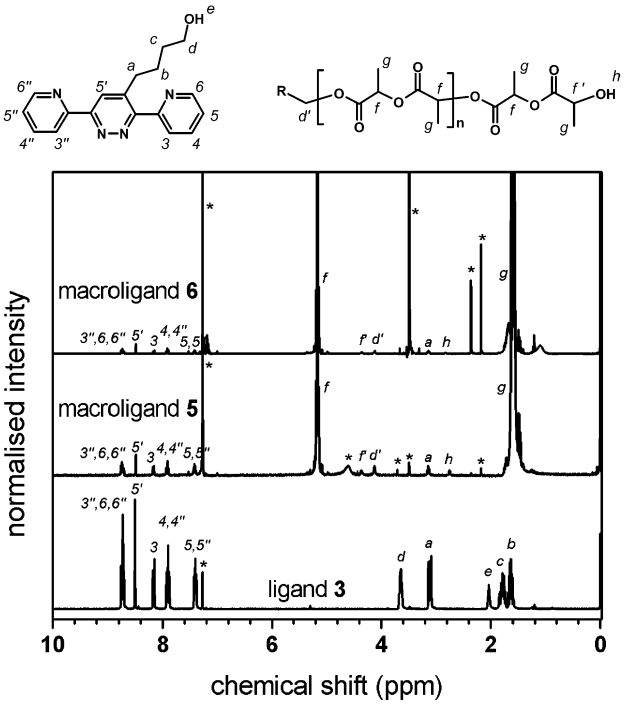

Figure 4. ^{1}H NMR spectra of ligand **3** and the macroligands **5** and **6** (chloroform-d_3). The stars represent residual solvents in the spectra.

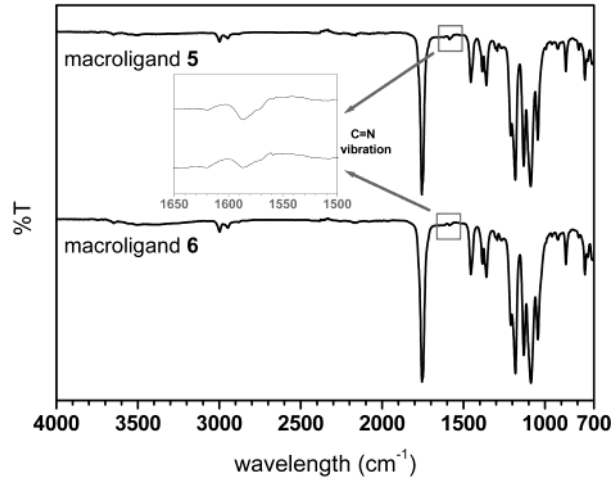

Figure 5. FT-IR spectra of the macroligands **5** and **6**. The inset shows the characteristic C=N stretch vibrations of the incorporated ligand.

Kricheldorf et al.[35,36] An aluminum alkoxide initiator was generated in situ from ligand **3** with 1 equiv of triethylaluminum (Scheme 2). Addition of different amounts of L-lactide to this initiator resulted in macroligands **5** and **6** ($M_{n,th}$ = 3900 Da and $M_{n,th}$ = 7500 Da, respectively). After precipitation in methanol, the resulting poly(L-lactide)s were characterized with ^{1}H NMR spectroscopy, infrared spectroscopy, and gel permeation chromatography (GPC). ^{1}H NMR spectra of ligand **3** and macroligands **5** and **6** (see Figure 4) clearly demonstrated the successful incorporation of the 3,6-bis(2-pyridyl)pyridazine ligand into the polymer chains: the aromatic signals of the heterocyclic protons are identical in the free ligand **3** and in the two polymers **5** and **6**, and the signal of the CH_2 protons next to the hydroxyl group of the ligand shifts from 3.72 to 4.12 ppm upon polymerization since the environment changes to an ester group. The integral ratios of the ligand (aromatic resonances) and the poly(L-lactide)s (5.2 and 1.2 ppm) revealed a number-average molecular weight ($M_{n,NMR}$) of 3840 Da for macroligand **5** and a $M_{n,NMR}$ of 6800 for macroligand **6** (Table 1). Both of these values are within 10% of the theoretical molecular weight, indicating that

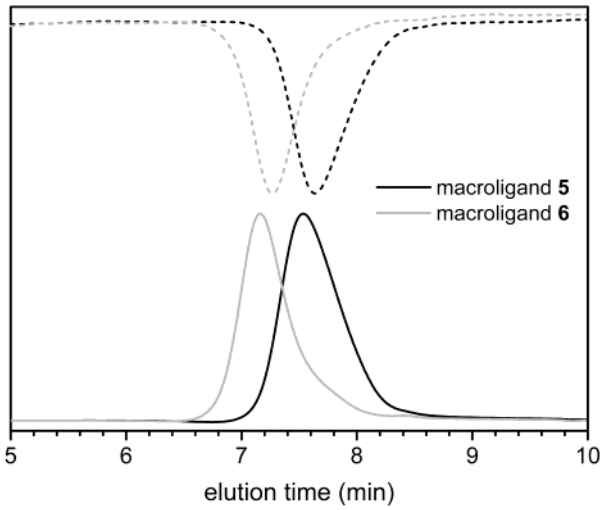

Figure 6. Normalized GPC traces of polymers **5** and **6** obtained with both the UV detector (254 nm, solid lines) and the RI detector (dotted lines) with chloroform as eluent.

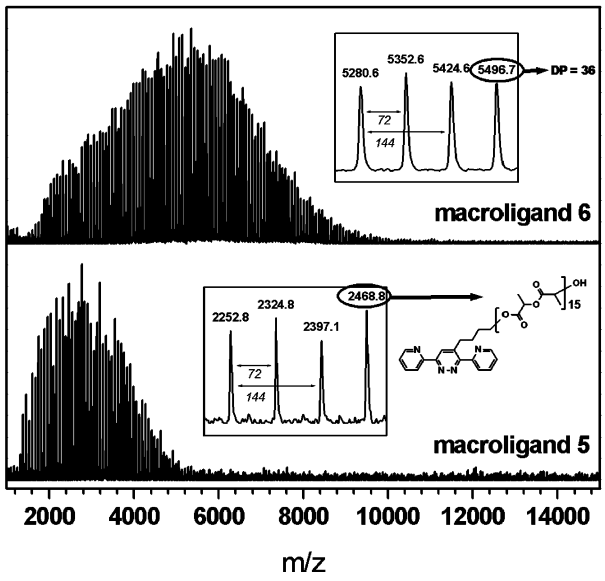

Figure 7. MALDI-TOF-MS spectra of both macroligands **5** and **6** obtained with dithranol as the matrix (without additional salt).

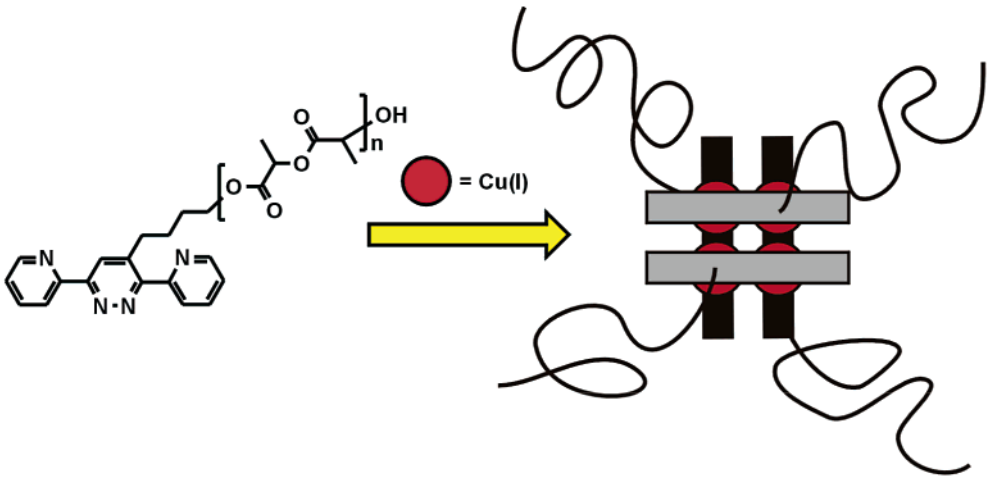

Figure 8. Schematic representation of the formation of polymeric gridlike complexes from the macroligands.

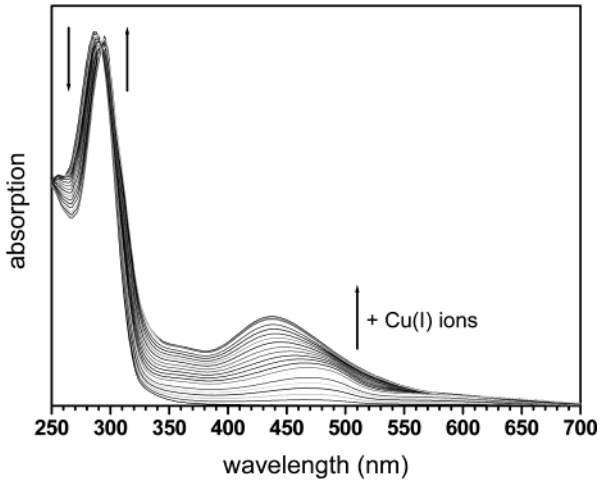

Figure 9. UV−vis titration of macroligand **6** with Cu(I)-$(CH_3CN)_4PF_6$ (dichloromethane). In each titration step 0.05 equiv of copper(I) ions relative to the macroligand is added.

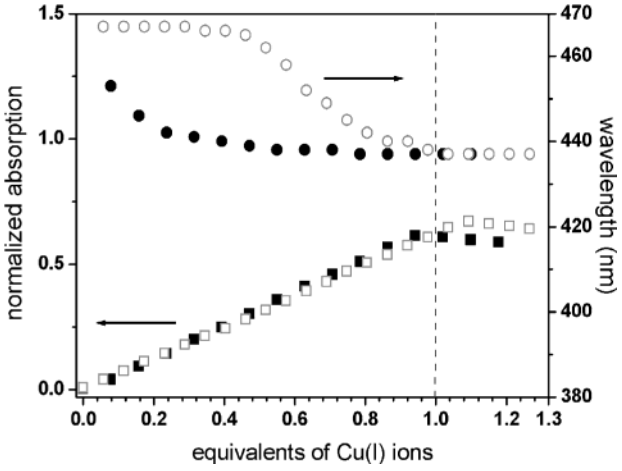

Figure 10. Graphical plot of the absorption at 437 nm from the macroligands **5** (■) and **6** (□) and the absorption maximum of the complexes formed from **5** (●) and **6** (○) vs the equivalents of Cu(I)$(CH_3CN)_4PF_6$ added.

the polymers were formed via a controlled polymerization mechanism. IR spectroscopy also revealed the successful incorporation of the ligand into the polymer chain: the C═N valence vibrations of the heterocycles at 1580 cm^{-1} are present in both polymers **5** and **6** (see inset of Figure 5). The signal is smaller for polymer **6** than for polymer **5** when the C═O stretch vibration for both polymers (1756 cm^{-1}) is kept constant, suggesting that the molecular weight of polymer **6** is higher. In addition, Figure **5** shows the presence of the characteristic bands for the poly(L-lactide)s at 2998 and 2948 cm^{-1} (CH_3 stretch vibrations), 1756 cm^{-1} (C═O stretch vibration), 1456 and 1360 cm^{-1} (CH_3 deformation), 1182 cm^{-1} (C−O stretch vibration), and at 1130, 1086, and 1044 cm^{-1} for the C−C vibrations. GPC characterization of the poly(L-lactide) macroligands was performed with chloroform as eluent utilizing both the UV detector (254 nm) and the refractive index (RI) detector. The macroligands were detected with both detectors (Figure 6), demonstrating that the ligand is incorporated into the polymer chains, since the poly(L-lactide) has no UV absorption at 254 nm. The GPC traces measure higher molecular weights than the ^1H NMR spectroscopic investigations for both macroligands (Table 1), which is probably because the GPC system was calibrated with polystyrene standards. Furthermore, the obtained polydispersity indices (PDI's) were around 1.20, which is indicative of a controlled polymerization.[37] Polymers **5** and **6** were also characterized with MALDI-TOF-MS (Figure 7). The obtained mass spectra revealed well-resolved signals that can be assigned to poly(L-lactide) chains containing the 3,6-bis(2-pyridyl)pyridazine moiety. The mass peaks correspond exactly to the masses calculated for single polymer chains with an additional proton (see insets of Figure 7). However, the presence of both even-membered and odd-membered oligomers implies that transesterification reactions occurred during the polymerization.[38] The molecular weights obtained for macroligands **5** and **6** from the MALDI-TOF-MS are significantly lower than those measured by ^1H NMR spectroscopy and GPC (Table 1). This is likely due to the overestimation of low-mass poly(L-lactide) chains because of their higher ionization probability.

Subsequently, the complexation of the poly(L-lactide) macroligands into polymeric grids (Figure 8) was studied with UV−vis spectroscopy. A stock solution of tetrakis(acetonitrile)copper(I) hexafluorophosphate in dichloromethane was titrated into solutions of the macroligands **5** and **6**. Upon addition of copper(I) salt, the color changed instantaneously due to the spontaneous self-assembly of the macroligands with copper(I) ions. After each titration step, a UV−vis spectrum was recorded in order to investigate the complexation behavior of the macroligands in detail. Figure 9 depicts

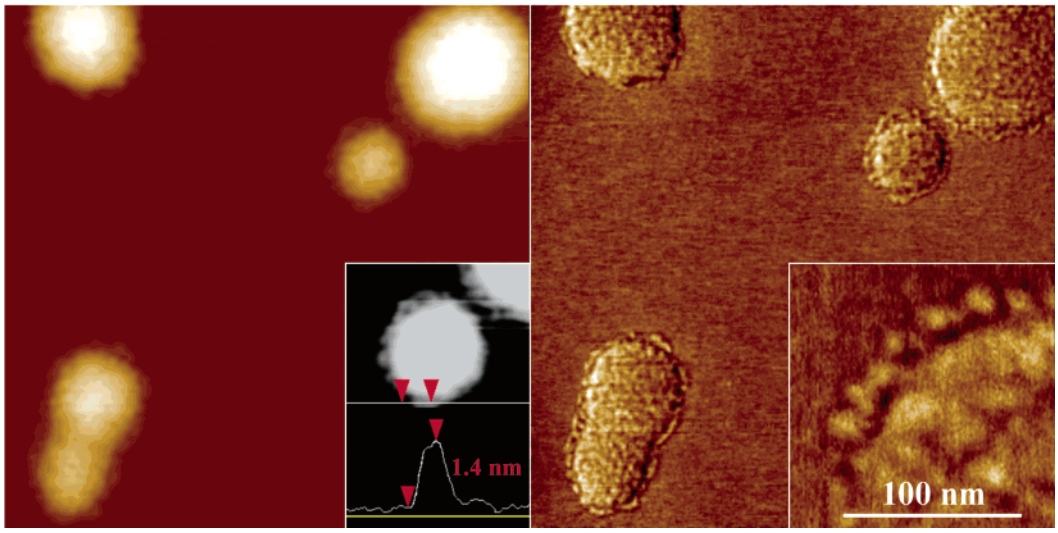

Figure 11. AFM height (left) and corresponding phase image (right) of clusters of the polymeric [2 × 2] grid based on compound **5** drop-casted onto mica (image size 1.33 μm). Left inset displays a line scan over isolated particles showing their height of 1.4 nm. Right inset displays a magnified phase image showing the lateral size of individual particles.

the UV−vis spectra obtained during the copper(I) titration of macroligand **6**. Upon addition of copper(I) ions an absorption band at 467 nm appeared. After the titration of approximately 0.6 equiv of copper(I) ions (regarding ligand molecules, a 1:1 ratio is expected for the grid formation), this absorption band shifted to 437 nm. The absorption at 437 nm is due to the formation of copper grids as already demonstrated for the complexation of nonpolymerized ligand **3**. Moreover, during the copper(I) addition, the ligand absorption at 288 nm decreased and an absorption band at 295 nm appeared. The resulting polymeric complex revealed similar absorption bands as the isolated gridlike complex **4** at 295 nm and at roughly 440 nm. During the titration of copper(I) ions to macroligand **5**, the absorption maximum shifted as well, although for this macroligand the shift occurred around the addition of 0.1 equiv of copper(I) ions. The resulting polymeric grids were soluble in dichloromethane, whereas the isolated supramolecular grid **4** precipitated in dichloromethane. This also demonstrated the incorporation of the grid complex into the polymers and showed clearly the new properties of the polymeric analogue. These results suggest a well-defined gridlike architecture for the polymeric [2 × 2] grids, which is comparable to the copper(I) grids described in the literature.

Figure 10 plots the UV−vis absorption at 437 nm (absorption maxima of the copper(I) complex) for both macroligands **5** and **6** against the equivalents of copper(I) ions added and also the change in absorption maximum during the addition of copper(I) ions.[39] For both macroligands, the absorption at 437 nm increased linearly upon addition of copper(I) salt, and the maximum absorption was obtained after approximately 1 equiv of copper(I) ions, demonstrating the formation of complete grids. Furthermore, the absorption maximum of macroligand **6** shifted from 467 to 437 nm around 0.6 equiv of copper(I) ions (Figure 10), which might suggest a transition from complexes with two ligands and one copper(I) ion into gridlike complexes with four ligands and four copper(I) ions. However, for macroligand **5** the absorption maximum shifted already from 453 to 437 nm around the addition of 0.1 equiv of copper(I) ions, suggesting that the longer polymer chains of macroligand **6** prevent the formation of grids more than the smaller polymer chains of macroligand **5**. This difference might be caused by decreased diffusion of copper(I) ions to the ligand and/or increased shielding effects resulting from the larger polymer chains present.

The polymeric [2 × 2] grids of macroligand **5** were also investigated with atomic force microscopy (AFM). A solution of the complex (0.05 mg/mL) was drop-cast onto mica and imagined utilizing tapping mode AFM. Clusters of single spherical particles piled up on each other surrounded by a corona of single particles were observed (Figure 11). These single particles have a height of 1.4 nm (Figure 11, left inset height image over a single particle). The inset of the phase image (right) shows a quarter of one of the large clusters, whereby both the single particles in the cluster and the corona of single particles around the cluster can be observed. The diameter (not corrected for the tip shape) of these single particles is 13−15 nm. The size of the single particles implies that they are individual grid-centered polymers (as shown in Figure 8), whereby the poly(lactide) chains are flattened on the surface, which is likely because they are attracted to the mica. In addition, AFM investigations of the free macroligand **5** onto mica did not show any special features, indicating that the structures found are indeed single polymeric [2 × 2] grids and clusters of these grids.

Attempts to characterize the polymer grids with GPC or MALDI-TOF-MS were unsuccessful, since the copper(I) metal complexes are not stable enough to survive the shear stress and the dilution in the GPC column or the ionization process in the MALDI-TOF-MS. The observed instability of the polymer grids was comparable with the isolated grid **4**. MALDI-TOF-MS of this isolated grid only revealed the free ligand and two ligands with one copper(I) ion. Similarly, reported ESI-MS of unsubstituted isolated grids showed only 8% of complete grids and many fragments.[23] Since for polymer mass spectrometry much higher laser intensities are required, it can be expected that the grids fall apart during the ionization process.

Conclusions

The successful Diels−Alder reaction between 3,6-bis-(2-pyridyl)tetrazine and 5-hexyn-1-ol, resulting in mono-

hydroxy-functionalized 3,6-bis(2-pyridyl)-4-hydroxybutylpyridazine, was reported. The complexation of this new functional ligand with copper(I) ions into gridlike complexes was demonstrated by utilizing UV−vis spectroscopy. Absorption bands at 295 and 440 nm were observed, which were also described for similar unfunctionalized gridlike complexes.

The potentials of such 3,6-bis(2-pyridyl)pyridazine ligands as supramolecular initiators were demonstrated by generating an aluminum alkoxide from this hydroxy-functionalized 3,6-bis(2-pyridyl)pyridazine, which acted as initiator for the controlled ring-opening polymerization of L-lactide. The resulting poly(L-lactide) macroligands with molecular weights of 3840 and 6800 Da were characterized with ^{1}H NMR spectroscopy, IR spectroscopy, gel permeation chromatography, and MALDI-TOF-MS, clearly revealing the incorporation of the ligand into the polymer chains and demonstrating that the macroligands were synthesized in a controlled way. The complexation with copper(I) ions was studied using UV−vis spectroscopy by a stepwise addition of tetrakis(acetonitrile)copper(I) hexafluorophosphate. During the addition of copper(I) ions, two stages were observed with different absorption maxima for the copper(I) grids. This might be due to transition from complexes with two ligands and one copper(I) ion to gridlike complexes with four ligands and four copper(I) ions. For the larger macroligand, the transition appeared at a higher concentration of copper(I) which suggests decreased diffusion of copper(I) ions to the ligand and/or increased shielding effects resulting from the larger polymer chains present.

AFM measurements showed the presence of clusters of polymer grids surrounded by a corona of single polymeric [2 × 2] grids. Further detailed investigations regarding structure, stability, and properties on these polymeric [2 × 2] grids are ongoing. The stability studies for these supramolecular polymers might result in switchable materials, whereby complexation or decomplexation can be induced by changing the environmental conditions.

Acknowledgment. The authors thank NWO, DPI, and the Fonds der Chemischen Industrie for financial support.

References and Notes

(1) Ramzi, A.; Prager, M.; Richter, D.; Efstratiadis, V.; Hadjichristidis, N.; Young, R. N.; Allgaier, J. B. *Macromolecules* **1997**, *30*, 7171−7182.
(2) Lee, S. C.; Chang, Y.; Yoon, J.-S.; Kim, C.; Kwon, I. C.; Kim, Y.-H.; Jeong, S. J. *Macromolecules* **1999**, *32*, 1847−1852.
(3) Gohy, J.-F.; Antoun, S.; Jérôme, R. *Macromolecules* **2001**, *34*, 7435−7440.
(4) Massey, J. A.; Winnik, M. A.; Manners, I.; Chan, V. Z.-H.; Ostermann, J. M.; Enchelmaier, R.; Spatz, J. P.; Moeller, M. *J. Am. Chem. Soc.* **2001**, *123*, 3147−3148.
(5) Heise, A.; Trollsås, M.; Magbitang, T.; Hedrick, J. L.; Frank, C. W.; Miller, R. D. *Macromolecules* **2001**, *34*, 2798−2804.
(6) Brunsveld, L.; Folmer, B. J. B.; Meijer, E. W.; Sijbesma, R. P. *Chem. Rev.* **2001**, *101*, 4071−4097.
(7) Schubert, U. S.; Eschbaumer, C. *Angew. Chem.* **2002**, *114*, 3016−3050; *Angew. Chem., Int. Ed.* **2002**, *41*, 2892−2926.
(8) Furue, M.; Umi, K.; Nozakura, S. I. *J. Polym. Sci., Polym. Lett. Ed.* **1982**, *20*, 291−295.
(9) Schubert, U. S.; Hofmeier, H. *Macromol. Rapid Commun.* **2002**, *23*, 561−566.
(10) Lavalette, A.; Hamblin, J.; Marsh, A.; Haddleton, D. M.; Hannon, M. J. *Chem. Commun.* **2002**, 3040−3041.
(11) Schubert, U. S.; Eschbaumer, C. *Macromol. Symp.* **2001**, *163*, 177−187.
(12) Lohmeijer, B. G. G.; Schubert, U. S. *Angew. Chem.* **2002**, *114*, 3980−3984; *Angew. Chem., Int. Ed.* **2002**, *41*, 3825−3829.
(13) Kaneko, M.; Nemoto, S.; Yamada, A.; Kurimura, Y. *Inorg. Chim. Acta* **1980**, *44*, L289−L290.
(14) Chujo, Y.; Sada, K.; Saegusa, T. *Macromolecules* **1993**, *26*, 6315−6319.
(15) Schubert, U. S.; Heller, M. *Chem.—Eur. J.* **2001**, *7*, 5252−5259.
(16) Wu, W.; Collins, J. E.; McAlvin, J. E.; Cutts, R. W.; Fraser, C. L. *Macromolecules* **2001**, *34*, 2812−2821.
(17) Heller, M.; Schubert, U. S. *Macromol. Symp.* **2002**, *177*, 87−96.
(18) Corbin, P. S.; Webb, M. P.; McAlvin, J. E.; Fraser, C. L. *Biomacromolecules* **2001**, *2*, 223−232.
(19) Fraser, C. L.; Smith, A. P. *J. Polym. Sci., Part A: Polym. Chem.* **2000**, *38*, 4704−4716.
(20) Lamba, J. J. S.; Fraser, C. L. *J. Am. Chem. Soc.* **1997**, *119*, 1801−1802.
(21) Hochwimmer, G.; Nuyken, O.; Schubert, U. S. *Macromol. Rapid Commun.* **1998**, *19*, 309−313.
(22) McAlvin, J. E.; Fraser, C. L. *Macromolecules* **1999**, *32*, 6925−6932.
(23) Youinou, M.-T.; Rahmouni, N.; Fischer, J.; Osborn, J. A. *Angew. Chem.* **1992**, *104*, 771−773; *Angew. Chem., Int. Ed. Engl.* **1992**, *31*, 775−778.
(24) Semenov, A.; Spatz, J. P.; Möller, M.; Lehn, J.-M.; Sell, B.; Schubert, D.; Weidl, C. H.; Schubert, U. S. *Angew. Chem.* **1999**, *111*, 2701−2705; *Angew. Chem., Int. Ed.* **1999**, *38*, 2547−2550.
(25) Baxter, P. N. W.; Lehn, J.-M.; DeCian, A.; Fischer, J. *Angew. Chem.* **1993**, *105*, 92−95; *Angew. Chem., Int. Ed. Engl.* **1993**, *32*, 89−90.
(26) Baxter, P. N. W.; Hanan, G. S.; Lehn, J.-M. *Chem. Commun.* **1996**, 2019−2020.
(27) Baxter, P. N. W.; Lehn, J.-M.; Fischer, J.; Youinou, M.-T. *Angew. Chem.* **1994**, *106*, 2432−2434; *Angew. Chem., Int. Ed. Engl.* **1994**, *33*, 2284−2287.
(28) Breuning, E.; Hanan, G. S.; Romero-Salguero, F. J.; Garcia, A. M.; Baxter, P. N. W.; Lehn, J.-M.; Wegelius, E.; Rissanen, K.; Nierengarten, H.; Van Dorsellaer, A. *Chem.—Eur. J.* **2002**, *8*, 3458−3466.
(29) Garcia, A. M.; Romero-Salguero, F. J.; Bassani, D. M.; Lehn, J.-M.; Baum, G.; Fenske, D. *Chem.—Eur. J.* **1999**, *5*, 1803−1808.
(30) Baxter, P. N. W.; Lehn, J.-M.; Baum, G.; Fenske, D. *Chem.—Eur. J.* **2000**, *6*, 4510−4517.
(31) Butte, W. A.; Case, F. H. *J. Org. Chem.* **1961**, *26*, 4690−4692.
(32) Meier, M. A. R.; Schubert, U. S. *Rapid Commun. Mass Spectrom.* **2003**, *17*, 713−716.
(33) Salditt, T.; An, Q.; Plech, A.; Eschbaumer, C.; Schubert, U. S. *Chem. Commun.* **1998**, 2731−2732.
(34) Weissbuch, I.; Baxter, P. N. W.; Cohen, S.; Cohen, H.; Kjaer, K.; Howes, P. H.; Als-Nielsen, J.; Hanan, G. S.; Schubert, U. S.; Lehn, J.-M.; Leiserowitz, L.; Lahav, M. *J. Am. Chem. Soc.* **1998**, *120*, 4850−4860.
(35) Kicheldorf, H. R.; Mang, T.; Jonté, J. M. *Macromolecules* **1984**, *17*, 2173−2181.
(36) Kricheldorf, H. R.; Kreiser-Saunders, I. *Macromol. Symp.* **1996**, *171*, 85−102.
(37) Mecerreyes, D.; Jérôme, R.; Dubois, P. *Adv. Polym. Sci.* **1999**, *147*, 1−59.
(38) Montaudo, G.; Montaudo, M. S.; Puglisi, C.; Samperi, F.; Spassky, N.; LeBrogne, A.; Wisniewski, M. *Macromolecules* **1996**, *29*, 6461−6465.
(39) The concentration of the macroligands was calculated with the molecular weight obtained from ^{1}H NMR spectroscopy.

MA034119E